POLITECNICO DI TORINO
Repository ISTITUZIONALE

Train-Track-Bridge Interaction Analytical Model with Non-proportional Damping: Sensitivity Analysis
and Experimental Validation

(Article begins on next page)

19 April 2024

# Train-track-bridge interaction analytical model with non-proportional damping: sensitivity analysis and experimental validation

Marco M. Rosso[1] [0000−0002−9098−4132], Angelo Aloisio[2] [0000−0002−6190−0139], Raffaele Cucuzza[1] [0000−0002−9344−6006], Giuseppe C. Marano[1] [0000−0001−8472−2956], and Rocco Alaggio[2] [0000−0003−4585−0108]

[1] Politecnico di Torino, DISEG, Dipartimento di Ingegneria Strutturale, Edile e Geotecnica, Corso Duca Degli Abruzzi, 24, Turin 10128, Italy, Email: marco.rosso@polito.it, raffaele.cucuzza@polito.it, giuseppe.marano@polito.it
[2] Università degli Studi dell'Aquila, via Giovanni Gronchi n.18, 67100 L'Aquila Email: angelo.aloisio1@univaq.it, rocco.alaggio@univaq.it

**Abstract.** Recent studies related to the dynamic response of railway bridges focused on gradually increasing the model complexity of the train-bridge interaction, however, did not always discuss any experimental validation. In the present work, the authors analyse the role of the ballast in the dynamic train-track-bridge interaction (TTBI). The analytical response of Euler-Bernoulli (EB) beams is coupled with a distributed springs layer modelling the ballast. The two equations are solved with trainloads as elementary moving load excitation, avoiding too complex models. This non-classically damped problem has been solved with a Runge-Kutta finite-difference method with temporal-spatial discretization. Furthermore, the authors experimentally validated the mathematical TTBI solution, comparing it with the displacement response of a case study. Specifically, at first, experimental modal bending stiffness parameters have been estimated to provide a representative equivalent EB beam model. Thereafter, the coupling effects of the ballast have been considered with a sensitivity analysis of the modelling parameters. Finally, the optimization to the actual experimental response of the model provided an estimate of the vertical ballast stiffness and its damping. The relevant difference in the damping of the experimental and mathematical model evidences the fundamental role of the ballast in adsorbing vibrations induced by the train passages.

**Keywords:** Railway Ballasts · Railway Bridge · Finite-Difference · Operational Modal Analysis.

# 1   Introduction

Ballasted track is the most widespread railway typology, consisting in the superstructure part (rails) and substructure one (ballast). Ballast is composed of natural or crushed coarse-sized, angular, crushed hard stone and rock uniformly graded. Retaining of the tracks and sleepers, stress propagation from tracks to subgrade and bearing functions, water drainage, etc. are only some of the most important functions accomplished by the ballast. The presence of the ballast produces changes in the boundary conditions and damping of the structure of medium spans railway bridges. Thus, many recent studies investigated the dynamic response of railway bridges under moving trains investigation. Many of them focused only on the train-bridge interaction modelling [1], concerning only about the type of trainload modeling (moving load, moving mass and moving spring-damper), or track modeling. Some simplified modeling techniques have been initially proposed based on beam or shell models of the bridge and track [2]. Nowadays, the actual tendency is to increase model complexity attempting to capture even complex phenomena. However, this involves high computational efforts, modeling errors and significant uncertainties. Therefore, further investigations on Train-Track-Bridge Interaction (TTBI) are essential in order to reduce model complexity which agree with experimental data validation [3]. Furthermore, to the authors knowledge, very few researches investigated the role of ballast in the bridge dynamic response. In the current study, the role of ballast is analysed and a simplified finite-difference formulation is adopted as modelling technique for the TTBI. The bridge and the track are modeled as Euler-Bernoulli beams coupled with a distributed springs layer to simulate the ballast, subjected to moving loads and solved by a Runge-Kutta finite difference method with spatial and temporal discretization.

# 2   TTBI coupled model formulation

## 2.1   Track model

The Euler-Bernoulli beam has been employed as the track model, denoting $w_r(x, t)$ as the deflection, $\rho_s A_r$ as constant mass per unit length, $\rho_s$ as the steel specific mass, $A_r$ as the rails cross-section area, $E_s I_r$ constant bending stiffness, $E_s$ as the steel Young's modulus and $I_r$ as the rails. The equation of motion can be written as: [2]

$$\rho_s A_r \ddot{w}_r(x, t) + E_s I_r w_{r,xxxx}(x, t) = q_r(x, t) + f_r(x, t) \tag{1}$$

in which $\ddot{w}$ and $w_{r,xxxx}$ respectively denotes the second time derivative and the fourth spatial coordinate $x$ derivative of $w$. The distributed load $q_r(x, t)$ arises from the springs bedding restraint to the track displacement:

$$q_r(x, t) = q_b(x, t) = k_f \left[ w_r(x, t) - w_b(x, t) \right] + c_f \left[ \dot{w}_r(x, t) - \dot{w}_b(x, t) \right] \tag{2}$$

denoting $k_f$ and $c_f$ as the stiffnesss and damping of the viscoelastic Winkler springs bedding, whereas $w_b$ is the bridge substructure deflection. $f_r(x, t)$ represents the effect of the

interaction forces between the rails and the vehicles. The train load has been modeled as moving concentrated uniformly spaced forces, in which each car is modeled by a single force, in a such way that a train of $N_v$ cars presents $N_v$ moving forces, labelled as $P_k$ with $k = 1, 2, \ldots, N_v$. Considering that the locomotive has a different weight $P_l$ with respect to the other cars $P_c$, then $P_k$ can be expressed as $P = \left\{ \frac{P_l}{2}, \left( \frac{P_l}{2} + \frac{P_c}{2} \right), P_c, \ldots, P_c, \ldots, P_c, \frac{P_c}{2} \right\}$. Assuming the first force enters the bridge at the initial time, the time of the $k$-th load entering the bridge can be expressed as $t_k = (k - 1)L_v/c$, $L_t$ is the train full length.

$$f_r(x, t) = \sum_{k=1}^{N_v} P_k \delta \left[ x - c(t - t_k) \right] \tag{3}$$

Denoting $L$ as the bridge length, the boundary conditions are expressed as follows for a pinned-pinned track:

$$w_r(0, t) = 0 \quad ; \quad w_{r,xx}(0, t) = 0 \quad ; \quad w_r(L, t) = 0 \quad ; \quad w_{r,xx}(L, t) = 0 \tag{4}$$

## 2.2  Bridge model

The bridge has been also modeled by Euler–Bernoulli beam, denoting $(\rho_c A_c + \rho_b A_b)$ as mass per unit length, $\rho_c$ as concrete specific mass of concrete, $A_c$ as the cross-section area of the beam, $\rho_b$ as the ballast specific mass, $A_b$ as the ballast cross-section area, $E_c I_c$ constant bending stiffness, with $E_c$ as concrete Young's modulus and $I_c$ as the beam cross-section inertia. The following partial differential equation describe the vertical bridge deflection $w_b(x, t)$ [4]:

$$(\rho_c A_c + \rho_b A_b)\ddot{w}_b(x, t) + E_c I_c w_{r,xxxx}(x, t) = q_b(x, t) \tag{5}$$

where $q_b(x, t)$ is the force that is transferred to the bridge via the springs bedding, defined as

$$q_b(x, t) = k_f \left[ w_b(x, t) - w_r(x, t) \right] + c_f \left[ \dot{w}_b(x, t) - \dot{w}_r(x, t) \right] \tag{6}$$

Since the bridge has a pinned-pinned scheme, the boundary conditions are the same of (4).

## 2.3  Spatial domain and time domain discretization

The TTBI model outlined in Figure 1 can be rewritten in matrix form considering the (1),(2),(5),(6) and, adopting the finite difference method, the beam domain is subdivided into $n$ intervals of $\Delta x$ length, thus obtaining the spatial discretization by approximating the fourth derivative. Denoting $I^{\{n \times n\}}$ and $0^{\{n \times n\}}$ as the identity and null matrices, $D_4^{\{n \times n\}}$ as the approximate fourth matrix derivative which satisfies the specific boundary conditions (4),
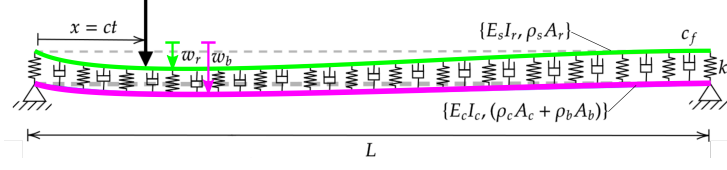
**Fig. 1.** Model of the TTBI.

$w_b(t)^{\{n\times1\}}$ and $w_r(t)^{\{n\times1\}}$ as the vertical deflection field of the bridge and track $f_r^{\{n\times1\}}$ as the discretized moving force vector described in 4, one obtains

$$
\begin{bmatrix} (\rho_c A_c + \rho_b A_b)\Delta x \boldsymbol{I} & \boldsymbol{0} \\ \boldsymbol{0} & \rho_s A_r \Delta x \boldsymbol{I} \end{bmatrix} \begin{Bmatrix} \ddot{w}_b(t) \\ \ddot{w}_r(t) \end{Bmatrix} + \begin{bmatrix} E_c I_c \boldsymbol{D}_4 - k_f \Delta x \boldsymbol{I} & k_f \Delta x \boldsymbol{I} \\ k_f \Delta x \boldsymbol{I} & E_s I_r \boldsymbol{D}_4 - k_f \Delta x \boldsymbol{I} \end{bmatrix} \begin{Bmatrix} w_b(t) \\ w_r(t) \end{Bmatrix} +
$$
$$
+ \begin{bmatrix} -c_f \Delta x \boldsymbol{I} & c_f \Delta x \boldsymbol{I} \\ c_f \Delta x \boldsymbol{I} & -c_f \Delta x \boldsymbol{I} \end{bmatrix} \begin{Bmatrix} \dot{w}_b(t) \\ \dot{w}_r(t) \end{Bmatrix} + \begin{Bmatrix} 0 \\ f_r \end{Bmatrix} = 0
$$

$$(7)$$

which, in compact form, is formally identical to the classical conventional dynamic problem

$$
\boldsymbol{M}\ddot{x}(t) + \boldsymbol{C}\dot{x}(t) + \boldsymbol{K}x(t) = \boldsymbol{f}(t) \tag{8}
$$

in which $\boldsymbol{M}^{\{2n\times2n\}}$, $\boldsymbol{C}^{\{2n\times2n\}}$ and $\boldsymbol{K}^{\{2n\times2n\}}$ denotes the mass, damping and stiffness matrices, $\boldsymbol{f}(t)$ is the generalized forcing term, and finally the generalized displacement field contains both bridge and track vertical deflections $x^{\{2n\times1\}} = \{w_b(t)^T, w_r(t)^T\}^T$. The following state-space model allowed performing the time domain discretization of (8):

$$
\dot{x}(t) = \boldsymbol{A}(t)x(t) + \boldsymbol{B}u(t) \tag{9}
$$

in which $x(t)$, $\boldsymbol{A}(t)$ and $\boldsymbol{B}$ and $u(t)$ are defined in [5] as function of the generalized mass, damping and stiffness matrices, and the forcing term. Thereafter, Tustin Approximation method from Matlab System Identification Toolbox provide the time discretized form, denoting $k$ as the time step, which has been solved using the Dormand-Prince method based on an explicit Runge-Kutta temporal discretization [6].

$$
\dot{x}_k = \boldsymbol{A}_k x_k + \boldsymbol{B}u_k \tag{10}
$$

## 3    Ballasted railway bridge case study and experimental campaign

Situated in the municipality of Trevi (Italy), the viaduct shown in Figure 2 presents 46 spans of about 20 m each, with 8 pre-tensioned longitudinal beams 1.40 m height and four transversal beams with 0.40x1.40 m rectangular cross-section. Accommodating two running tracks, the
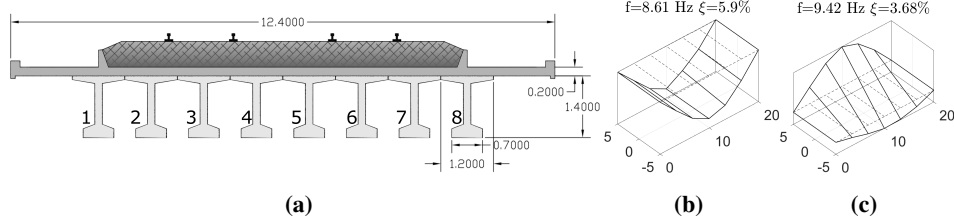
**Fig. 2.** Cross-section details with beams numbering and first two experimental mode shapes.

**Table 1.** Optimum parameters of an equivalent EB beam model and comparison in terms of natural frequency and Modal Assurance Criterion (MAC).

| $f_{\text{exp}}$ [Hz] | $f_{\text{theo}}$ [Hz] | MAC [%] | $\frac{f_{\text{exp}} - f_{\text{theo}}}{f_{\text{exp}}}$ [%] | $EI_{\text{b,opt}}$ [kNmm$^2$] |
|---|---|---|---|---|
| 8.61 | 8.62 | 92 | -0.12 | 12600 |

concrete slab is 20 cm thick with lateral side walkways cantilever of 1.40 m, leading to about 12.40 m the total deck width. The piers are mainly characterized by 11.00x1.50 m pseudo-rectangular reinforced concrete walls, with pier caps presenting an enlargement of 30 cm around the pier shape and an average height of 50 cm. Operational dynamic identification of the bridge has been performed with 7 equally spaced Force Balance Accelerometers (FBA) with 3.30 m steps and with the two extremal ones placed in the nearby of the supports. Two measurement chains have been performed connected by a master recording unit, providing 20 minutes recordings sampled at a rate of 200 Hz. Operational modal analysis (OMA) with covariance-driven Stochastic Subspace Identification (SSI) method have been performed, clearly identifying three stable modes in the range 0-40 Hz [7]. The outcomes showed that the bridge exhibits both bending and torsional modes which are not coupled, as depicted in Fig.2. Therefore, the first bending mode can be reasonably adopted to estimate the bending stiffness $EI_b$ of an equivalent pinned-pinned beam model by solving a nonlinear least-squares problem [8]:

$$\hat{\theta} = \arg\min_{\theta} J(\theta) = \arg\min_{\theta} \sum_i w_{\epsilon,i} \left( \epsilon_{z,i}(\theta) \right)^2 \tag{11}$$

$$\epsilon_{\lambda_i}(\theta) = \frac{\lambda_i(\theta) - \tilde{\lambda}_i}{\tilde{\lambda}_i} | i \in \{1 - n\} \tag{12}$$

with $w_{\epsilon,i}$ as a weighting factor, assumed $w_{\epsilon,i} = 1$ for simplicity, $\epsilon_{z,i}$ as the residuals between the experimental and numerical modal data $z$, considering the undamped eigenvalue $z = \lambda$ with $\lambda_i = (2\pi f_i)^2$, where $f$ is the natural frequency, whereas the tilde denotes experimental values. The final optimum outcome results in $EI_b \approx 12600$ kNmm$^2$, as illustrated in Tab.1.
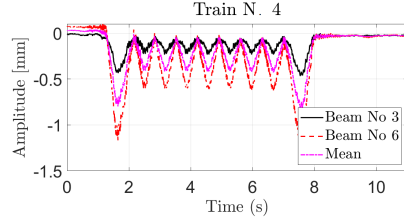
**Fig. 3.** Displacement response of the bridge under the moving train N.4.

Two micro-epsilon optoNCDT 1420 laser sensors of 1000 Hz sampling rate have been adopted for vertical displacements of the 3rd and 6th beam soffit monitoring during four train passages. Since the train weight is known only in Train N.4, only that measurement have been reported in Fig.3 and thus the sensitivity analysis have been conducted based on those data. By inspecting the experimental data, after train passages, steady-state oscillations are not present, probably due to the high damping of the ballasted track. The displacement trend could be decomposed into a constant stationary response due to the general beam deflection and an oscillatory one related to the passage of the axes. The different response of the 3rd and 6th beam evidences a torsional response, which has been purged reconducting to an average response due to the EB modelling considered in the present work. The first and last peak responses are more evident due to the higher locomotive weight with respect to the other cars.

## 4   Univariate and multivariate covariance-based sensitivity analysis

Before estimating the optimal model parameters for the proposed finite difference approximation which most agree with experimental data, the rank correlation coefficient [9] was inspected to evaluate the similarity degree between experimental $\boldsymbol{x}_m$ and simulated $\boldsymbol{x}_s$ displacement response:

$$\mathrm{corr}(\boldsymbol{x}_s, \boldsymbol{x}_m) = \frac{\boldsymbol{x}_s \cdot \boldsymbol{x}_m}{|\boldsymbol{x}_s| \cdot |\boldsymbol{x}_m|} \tag{13}$$

with $(\cdot)$ as the inner product and $|\ |$ as the norm operator. The sensitivity involved the parameters in Tab.2 such as ballast, the bending stiffness of the beam and the train velocity, which are characterized by a certain range of variation (see Tab.2). This allow to explore the ballast contribution and assess the effect of the modelling choices. Since the ballast stiffness value is still nowadays discussed, the authors identify a reasonable interval between 60 MPa, assuming an estimate of the Winkler coefficient for compacted gravel, and 600 Mpa, obtained by an order of magnitude greater the lower bound. Even for the non-proportional damping coefficient ($c_f$) there is no a general consensus about the range of variation, however some

**Table 2.** List of the parameters chosen for the sensitivity analysis and range of variations.

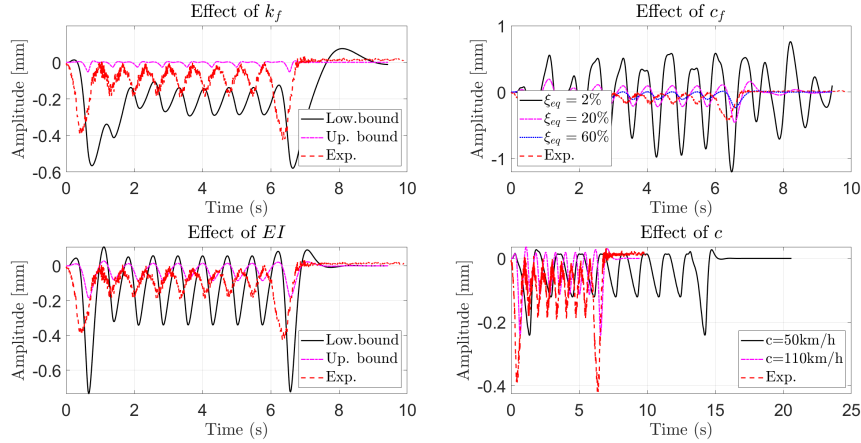| Parameters | Symbol | Lower bound | Upper bound |
|---|---|---|---|
| Vertical stiffness of the ballast [MPa] | $k_f$ | 60 | 600 |
| Damping coefficient of the ballast [MPa s] | $c_f$ | 0.1 | 100 |
| Bending stiffness of the bridge [kNmm$^2$] | $E_cI_c$ | $(1-50\%)EI_{b,\text{opt}}$ | $(1+50\%)EI_{b,\text{opt}}$ |
| Velocity of the train [km/h] | c | 50 | 200 |



**Fig. 4.** Qualitative results of monovariate sensitivity analyses.

trial tests attempted to compare the non-proportional damped response with an equivalent damping ratio $\xi_{eq}$, proportional to the mass and stiffness matrix:

$$c_{f,\text{lower}} \approx 0.1\text{Mpa}/s \rightarrow \xi_{eq} \approx 10\% \quad ; \quad c_{f,\text{upper}} \approx 20\text{Mpa}/s \rightarrow \xi_{eq} \approx 200\% \qquad (14)$$

Notwithstanding, the damping upper bound might seem an overestimation, however, in ballasted tracks, non-proportional damping may sometimes lead to super-critical damping conditions. The bending stiffness range is obtained by lowering or increasing the optimum bending stiffness found from deterministic model updating using the first experimental natural frequency. Considering railways standards velocity limits, the train velocity range vary between 30 and 200 km/h. A monovariate sensitivity analysis have been performed and the effects on the displacement response qualitative depicted Fig.4. Focusing on the vertical stiffness, when $k_f$ is low the train acts as a concentrated load, instead, on the other hand, it produces a greater load distribution which affects both amplitude and the delay of the response. The effects produced when the damping $c_f$ is low ($\xi_{eq} \approx 20\%$) are related to a growth in the amplitude response, whereas when it is high it produces a higher reduction of the displacement response after the first oscillation. Thus, when a sequence of different train loads occurs, the response

**Table 3.** Results of the multivariate sensitivity analysis.

| Parameters | Peak displacement | | Rank correlation coefficient | |
|---|---|---|---|---|
| Sensitivity indicators | $S_1$ [%] | $S_T$ [%] | $S_1$ [%] | $S_T$ [%] |
| Vertical stiffness of the ballast | 38.56 | 41.34 | 39.72 | 39.61 |
| Damping coefficient of the ballast | 20.31 | 22.34 | 33.65 | 34.67 |
| Bending stiffness of the bridge | 40.26 | 45.12 | 38.23 | 39.34 |
| Velocity of the train | 0.89 | 1.23 | / | / |
| Sum | 100.02 | 110.03 | 111.6 | 113.62 |

corresponds to a quasi-static loading preventing the beam oscillations. The bending stiffness $EI$ only affects the amplitude of the displacement response and does not impact significantly the response delay. Since the train velocity $c$ mainly affects the amplitude response due to inertial effects and the duration of the time series, it has been removed in the sensitivity analysis of the rank correlation coefficient.

A successive multivariate sensitivity analysis has permitted to decompose the variance of the output of the model (peak displacement and objective function) into fractions which can be attributed to the chosen parameters [10]. Foremost, considering the inputs sampling range in Tab.2, inputs were generated according to the Saltelli's sampling scheme. Specifically, given $N = 100$ number of samples and $D = 4$ number of input parameters, $(N \cdot (2D + 2))$ models were generated. After all the models were analysed, the first-order $S_1$ and total-order $S_T$ sensitivity indices were calculated. These two quantities estimates the effect of varying a single parameter only and the contribution to the output variance of the selected parameter including all variance caused by its interactions with the other parameters, respectively. Two separate analysis have been performed related to the peak displacement evaluation and the rank correlation coefficient, as shown in Tab.3. In conclusion, $k_f$ and $EI$ manifest the most significant influences with sensitivity indices about 40%. Even the ballast damping coefficient exhibits quite important sensitivity indicators about 20%. The train velocity exhibits negligible effects, as remarked by [4]. The correspondence of the results between $S_1$ and total-order $S_T$ proves that the selected parameters are substantially uncorrelated, thus they can be adopted for global optimization avoiding an overdetermined problem.

## 5    Model updating optimization procedure

To calibrate the stiffness and damping parameters of the ballasted track, the following optimization problem was solved adopting the genetic algorithm (GA) [11,12] from Matlab global optimization toolbox:

$$\hat{X} = \arg \min_{X} \text{corr}(\boldsymbol{d}_{s,s}, \boldsymbol{d}_{s,m}) \tag{15}$$
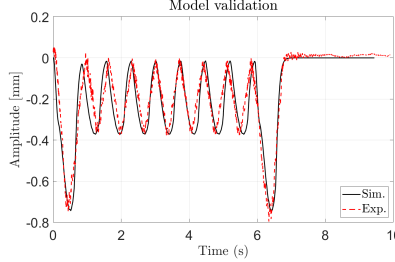
**Fig. 5.** Comparison between the experimental and simulated displacement response obtained with the optimized parameters.

$$\text{obj}(\mathbf{p}) = \frac{\sum_{i=1}^{N} |\left[w_{b,ei} - w_{b,si}(\mathbf{p})\right] \Delta t_i|}{\sum_{i=1}^{N} |w_{b,ei} \Delta t_i|} \tag{16}$$

where $N$ is the number of data points, $\mathbf{p}$ is the design vector containing the parameters to be optimized, $w_{b,ei}$ is the experimental deflection of the bridge, $w_{si}(\mathbf{p})$ is the simulated beam deflection and $\Delta t_i$ is the time integration step. The objective function (OF) formulation is a normalized integral of the difference between experimental and simulated response. The parameters' lower and upper bounds are shown in Tab.2. To improve the convergence, as explained in Sec.3, $EI_b$ was set to 12600 kNmm$^2$. The train speed is not included in the updating, however it was estimated from the video recording of the train passage. Since the train weight was known only in the train N.4 (Fig.3) the optimization has been limited to that record, finding the following optimal solution: $\boldsymbol{p}_{opt} = \{k_f, c_f\} = \{490.49\,\text{Mpa}, 14.50\,\text{Mpa}\cdot s\}$. In Fig.5, the final simulated solution from the finite difference model shows a good agreement with experimental response. $k_f$ reaches an optimum almost 80 times the expected value for compacted gravel, whereas $c_f$ is close to 14 Mpa·s, thus an equivalent damping ratio close to 100%. To the authors' knowledge, no one attempted to estimate $k_f$ and $c_f$ with model updating of the experimental displacement response. However, [3] achieved good results by using an EB beam without the ballast, optimizing the bending stiffness but not providing an estimate of $k_f$ and $c_f$ using the experimental data.

## 6   Conclusions

The current study presents the mathematical framework for finite difference model of the Train-Track-Bridge interaction (TTBI). The model is based on coupling effects of Euler-Bernoulli beams representing the track and the bridge and a distributed layer of springs and dashpots modeling the ballast. In literature, many studies focused on very complex models to consider ballast interaction, however very few experimental validations have been carried our. The authors focused on a prestressed concrete ballasted railway bridge case study, monitoring

the displacement response under moving trains. The standard dynamic identification under environmental vibrations have been carried out to estimate the bending stiffness of the bridge. Thereafter, a variance-based sensitivity analysis of the peak displacement response and the rank correlation coefficient proves that both the ballast mechanical properties and the bridge bending stiffness affect the displacement response. Finally, a model updating procedure have been carried out to optimize the ballast parameters based on experimental displacement response data adopting the proposed finite difference model. The ballast optimal vertical stiffness approaches to 400Mpa, whereas optimal non-proportional damping reaches about 14 Mpa·s. Future developments may include some more sophisticated modeling of the trainload, e.g. moving mass-spring-damper, in order to assess if further model complexity is actually beneficial for assessing the mechanical characteristics of the ballasted track.

# References

1. Xia, H., Zhang, N., Guo, W.: Dynamic interaction of train-bridge systems in high-speed railways. Springer, Berlin, Germany, DOI 10, 978–3 (2018)
2. Di Lorenzo, S., Di Paola, M., Failla, G., Pirrotta, A.: On the moving load problem in euler–bernoulli uniform beams with viscoelastic supports and joints. Acta Mechanica 228(3), 805–821 (2017)
3. Feng, D., Feng, M.Q.: Model updating of railway bridge using in situ dynamic displacement measurement under trainloads. Journal of Bridge Engineering 20(12), 04015019 (2015)
4. Frỳba, L.: Vibration of solids and structures under moving loads, vol. 1. Springer Science & Business Media (2013)
5. Craig Jr, R.R., Kurdila, A.J.: Fundamentals of structural dynamics. John Wiley & Sons (2006)
6. Dormand, J.R., Prince, P.J.: A family of embedded runge-kutta formulae. Journal of computational and applied mathematics 6(1), 19–26 (1980)
7. Aloisio, A., Pasca, D.P., Battista, L., Rosso, M.M., Cucuzza, R., Marano, G., Alaggio, R.: Indirect assessment of concrete resistance from fe model updating and young's modulus estimation of a multi-span psc viaduct: Experimental tests and validation. Structures 37, 686–697 (01 2022)
8. He, L., Castoro, C., Aloisio, A., Zhang, Z., Marano, G.C., Gregori, A., Deng, C., Briseghella, B.: Dynamic assessment, fe modelling and parametric updating of a butterfly-arch stress-ribbon pedestrian bridge. Structure and Infrastructure Engineering pp. 1–12 (2021)
9. Aloisio, A., Alaggio, R., Fragiacomo, M.: Bending stiffness identification of simply supported girders using an instrumented vehicle: Full scale tests, sensitivity analysis, and discussion. Journal of Bridge Engineering 26(1), 04020115 (2021)
10. Pasca, D.P., Aloisio, A., Fragiacomo, M., Tomasi, R.: Dynamic characterization of timber floor subassemblies: Sensitivity analysis and modeling issues. Journal of Structural Engineering 147(12), 05021008 (2021)
11. Cucuzza, R., Rosso, M.M., Marano, G.: Optimal preliminary design of variable section beams criterion. SN Applied Sciences 3 (08 2021)
12. Cucuzza, R., Costi, C., Rosso, M.M., Domaneschi, M., Marano, G., Masera, D.: Optimal strengthening by steel truss arches in prestressed girder bridges. Proceedings of the Institution of Civil Engineers - Bridge Engineering pp. 1–51 (01 2022)